Biogeosciences Discuss., https://doi.org/10.5194/bg-2018-241
Manuscript under review for journal Biogeosciences
Discussion started: 13 June 2018

Microbial decomposition processes and vulnerable Arctic soil organic carbon in the 21st century

Junrong Zha and Qianlai Zhuang

Department of Earth, Atmospheric, and Planetary Sciences and Department of Agronomy,
Purdue University, West Lafayette, IN 47907 USA

Correspondence to: qzhuang@purdue.edu

Biogeosciences Discuss., https://doi.org/10.5194/bg-2018-241
Manuscript under review for journal Biogeosciences
Discussion started: 13 June 2018

Abstract

Inadequate representation of biogeochemical processes in current biogeochemistry models contributes to a large uncertainty in carbon budget quantification. Here, detailed microbial mechanisms were incorporated into a process-based biogeochemistry model, the Terrestrial Ecosystem Model (TEM). Ensemble regional simulations with the model estimated the carbon budget of the Arctic ecosystems is 76.0 ±114.8 Pg C during the 20th century, -3.1 ±61.7 Pg C under the RCP 2.6 scenario and 94.7 ±46 Pg C under the RCP 8.5 scenario during the 21st century. Positive values indicate the regional carbon sink while negative values are source to the atmosphere. Compared to the estimates using a simpler soil decomposition algorithm in TEM, the new model estimated that the Arctic terrestrial ecosystems stored 12 Pg less carbon over the 20th century, 19 Pg C and 30 Pg C less under the RCP 8.5 and RCP 2.6 scenarios, respectively, during the 21st century. When soil carbon within depths 30 cm, 100 cm and 300 cm was considered as initial carbon in the 21st century simulations, the region was estimated to accumulate 65.4, 88.6, and 109.8 Pg C, respectively, under the RCP 8.5 scenario. In contrast, under the RCP 2.6 scenario, the region lost 0.7, 2.2, and 3 Pg C, respectively, to the atmosphere. We conclude that the future regional carbon budget evaluation largely depends on whether or not the adequate microbial activities are represented in earth system models and the sizes of soil carbon considered in model simulations.

Biogeosciences Discuss., https://doi.org/10.5194/bg-2018-241
Manuscript under review for journal Biogeosciences
Discussion started: 13 June 2018

1. Introduction

Northern high-latitude soils and permafrost contain more than 1,600 Pg carbon (Tarnocai et al 2009). Climate over this region has warmed in recent decades (Serreze and Francis 2006) and the increase is 1.5 to 4.5 times the global mean (Holland and Bitz 2003). Warming-induced changes in carbon cycling are expected to exert large feedbacks to the global climate system (Davidson and Janssens 2006, Christensen and Christensen 2007, Oechel et al 2000).

Warming is expected to accelerate soil C loss by increasing soil respiration, but increasing nutrient mineralization, thereby stimulating plant net primary production (NPP) (Mack et al 2004, Hobbie et al 2002). Thus, the variation of climate may switch the role of the Arctic system between a C sink and a source if soil C loss overtakes NPP (Davidson et al 2000, Jobb ágy and Jackson 2000). Process-based biogeochemical models such as TEM (Hayes et al 2014, Raich and Schlesinger 1992, McGuire et al 1992, Zhuang et al 2001, 2002, 2003, 2010, 2013), Biome-BGC (Running and Coughlan 1988), CASA (Potter et al 1993), CENTURY (Parton et al 1994) and Biosphere Energy Transfer Hydrology scheme (BETHY) (Knorr et al 2000) have been widely used to quantify the response of carbon dynamics to climatic changes (Todd-Brown et al 2012). An ensemble of process-based model simulations suggests that arctic ecosystems acted as a sink of atmospheric CO_2 in recent decades (McGuire et al 2012, Schimel et al 2013). However, the response of this sink to increasing levels of atmospheric CO_2 and climate change is still uncertain (Todd-Brown et al 2013). The IPCC 5th report also shows that land carbon storage is the largest source of uncertainty in the global carbon budget quantification (Ciais et al 2013).

Much of the uncertainty is also due to the inadequate representation of ecosystem processes that determine the exchanges of water, energy and C between land ecosystems and the atmosphere (Wieder et al 2013), and ignorance of some key biogeochemical mechanisms (Schmidt et al 2011). For example, heterotrophic respiration (R_H) is the primary loss pathway for soil organic carbon (Hanson et al 2000, Bond-Lamberty and Thomson 2010). and it generally increases with increasing temperature (Davidson and Janssens 2006) and moisture levels in well-drained soils (Cook and Orchard 2008). Moreover, this process is closely related to soil nitrogen mineralization that determines soil N availability and affects gross primary production (Hao et al 2015). To date, most models treated soil decomposition as a first-order decay process, i.e., CO_2 respiration is directly proportional to soil organic carbon. However, it is not clear if these models are robust under changing environmental conditions (Lawrence et al 2011, Schimel and Weintraub 2003, Barichivich et al 2013) since they often ignored the effects of changes in biomass and composition of decomposers, while recent empirical studies have shown that microbial abundance and community play a significant role in soil carbon decomposition (Allison and Martiny 2008). The control that microbial activity and enzymatic kinetics imposed on soil respiration suggests the need for explicit representation of microbial physiology, enzymatic activity, in addition to the direct effects of soil temperature and soil moisture on heterotrophic respiration (Schimel and Weintraub 2003). Recent mechanistically-based models explicitly incorporated with the microbial dynamics and enzyme kinetics that catalyze soil C decomposition have produced notably different results and a closer match to contemporary observations (Wieder et al 2013, Allison et al 2010) indicating the need for incorporating these

microbial mechanisms into large-scale earth system models to quantify carbon dynamics under future climatic conditions ((Wieder et al 2013, Allison et al 2010).

This study advanced a microbe-based biogeochemistry model (MIC-TEM) based on an extant Terrestrial Ecosystem Model (TEM) (Raich and Schlesinger 1992, McGuire et al 1992, Zhuang et al 2001, 2002, 2003, 2010, 2013, Hao et al 2015). In MIC-TEM, the heterotrophic respiration is not only a function of soil temperature, soil organic matter (SOM) and soil moisture, but also considers the effects of dynamics of microbial biomass and enzyme kinetics (Allison et al 2010). The verified MIC-TEM was used to quantify the regional carbon dynamics in northern high latitudes (north 45 °N) during the 20th and 21st centuries.

2. Methods

2.1 Overview

Below we first briefly describe how we advanced the MIC-TEM by modifying the soil respiration process in TEM (Zhuang et al 2003) to better represent carbon dynamics in terrestrial ecosystems. Second, we describe how we parameterized and verified the new model using observed net ecosystem exchange data at representative sites and how simulated net primary productivity (NPP) was evaluated with Moderate Resolution Imaging Spectroradiometer (MODIS) data to demonstrate the reliability of new model at regional scales. Third, we present how we applied the model to the northern high latitudes for the 20th and 21st centuries. Finally, we introduce how we conducted the sensitivity analysis on initial soil carbon input, using gridded observation-based soil carbon data of three soil depths during the 21st century.

Biogeosciences Discuss., https://doi.org/10.5194/bg-2018-241
Manuscript under review for journal Biogeosciences
Discussion started: 13 June 2018

111 **2.2 Model description**

112 TEM is a highly aggregated large-scale biogeochemical model that estimates the dynamics of
113 carbon and nitrogen fluxes and pool sizes of plants and soils using spatially referenced
114 information on climate, elevation, soils and vegetation (Raich and Schlesinger 1992, McGuire et
115 al 1992, Zhuang et al 2003, 2010, Melillo et al 1993). To explicitly consider the effects of
116 microbial dynamics and enzyme kinetics on large-scale carbon dynamics of northern terrestrial
117 ecosystems, we developed MIC-TEM by coupling version 5.0 of TEM (Zhuang et al 2003, 2010)
118 with a microbial-enzyme module (Hao et al 2015, Allison et al 2010). Our modification of the
119 TEM improved the representation of the heterotrophic respiration (R_H) from a first-order
120 structure to a more detailed structure (Fig. S1).

121 In TEM, heterotrophic respiration R_H is calculated as a function of soil organic carbon
122 (SOC), soil temperature (Q_{10}), soil moisture (f (MOIST)), and the gram-specific decomposition
123 constant K_d:

124 $$R_H = K_d * SOC * Q_{10}^{\frac{DT}{10}} * f(MOIST) \quad (1)$$

125 where DT is soil temperature at top 20 cm. CO_2 production from SOC pool is directly
126 proportional to the pool size, and the activity of decomposers only depends on the built-in
127 relationships with soil temperature and moisture (Todd-Brown et al 2012). Therefore, the
128 changes in microbial community composition or adaption of microbial physiology to new
129 conditions were not represented in TEM. However, current studies indicate that soil C
130 decomposition depends on the activity of biological communities dominated by microbes
131 (Schimel and Weintraub 2003), implying that the biomass and composition of the decomposer
132 community can't be ignored (Todd-Brown et al 2012).

Biogeosciences Discuss., https://doi.org/10.5194/bg-2018-241
Manuscript under review for journal Biogeosciences
Discussion started: 13 June 2018

We thus revised the first-order soil C structure in TEM to a second-order structure considering microbial dynamics and enzyme kinetics according to Allison et al 2010. In MIC-TEM, heterotrophic respiration (R_H) is calculated as:

$$R_H = ASSIM*(1-CUE) \quad (2)$$

Where ASSIM and CUE represent microbial assimilation and carbon use efficiency, respectively. ASSIM is modeled with a Michaelis-Menten function:

$$ASSIM = Vmax_{uptake} * MIC * \frac{DOC}{Km_{uptake}+DOC} \quad (3)$$

Where $Vmax_{uptake}$ is the maximum velocity of the reaction and calculated using the Arrhenius equation:

$$Vmax_{uptake} = Vmax_{uptake_0} * e^{-\frac{Ea_{uptake}}{R*(temp+273)}} \quad (4)$$

$Vmax_{uptake_0}$ is the pre-exponential coefficient, Ea_{uptake} is the activation energy for the reaction ($Jmol^{-1}$), R is the gas constant (8.314 $Jmol^{-1}K^{-1}$), and temp is the temperature in Celsius under the reaction occurs.

Besides, Km_{uptake} value is calculated as a linear function of temperature:

$$Km_{uptake} = Km_{uptake_{slope}} * temp + Km_{uptake_0} \quad (5)$$

Microbial biomass MIC is modeled as:

$$\frac{dMIC}{dt} = ASSIM * CUE - DEATH - EPROD \quad (6)$$

Where microbial biomass death (DEATH) and enzyme production (EPROD) are modeled as constant fraction of microbial biomass:

$$DEATH = r_{death} * MIC \quad (7)$$

$$EPROD = r_{EnzProd} * MIC \quad (8)$$

Biogeosciences Discuss., https://doi.org/10.5194/bg-2018-241
Manuscript under review for journal Biogeosciences
Discussion started: 13 June 2018

Where r_{death} and $r_{EnzProd}$ are the ratio of microbial death and enzyme production, respectively.

Dissolved organic carbon (DOC) is part of soil organic carbon:

$$\frac{\mathrm{dDOC}}{\mathrm{dt}} = \mathrm{DEATH} * (1 - \mathrm{MICtoSOC}) + \mathrm{DECAY} + \mathrm{ELOSS} - \mathrm{ASSIM} \quad (9)$$

where MICtoSOC is carbon input as dead microbial biomass to SOC, representing the fraction of microbial death that flows into SOC, and is set as a constant value according to Allison et al 2010. SOC dynamics are modeled:

$$\frac{\mathrm{dSOC}}{\mathrm{dt}} = \mathrm{Litterfall} + \mathrm{DEATH} * \mathrm{MICtoSOC} - \mathrm{DECAY} \quad (10)$$

Where Litterfall is estimated as a function of vegetation carbon (Zhuang et al 2010). The enzymatic decay of SOC is calculated as:

$$\mathrm{DECAY} = \mathrm{V_{max}} * \mathrm{ENZ} * \frac{\mathrm{SOC}}{Km + \mathrm{SOC}} \quad (11)$$

Where V_{max} is the maximum velocity of the reaction and calculated using the Arrhenius equation:

$$V_{max} = \mathrm{Vmax_0} * \mathrm{e}^{-\frac{Ea}{\mathrm{R}*(\mathrm{temp}+273)}} \quad (12)$$

The parameters Km and carbon use efficiency (CUE) are temperature sensitive, and calculated as a linear function of temperature between 0 and 50 ℃:

$$Km = \mathrm{Km}_{slope} * \mathrm{temp} + \mathrm{Km_0} \quad (13)$$

$$\mathrm{CUE} = \mathrm{CUE_{slope}} * \mathrm{temp} + \mathrm{CUE_0} \quad (14)$$

Where CUEslope and CUE_0 are parameters for calculating CUE. The values of $\mathrm{CUE_{slope}}$ and $\mathrm{CUE_0}$ were derived from Allison et al 2010.

ELOSS is also a first-order process, representing the loss of enzyme:

$$\mathrm{ELOSS} = \mathrm{r_{enzloss}} * \mathrm{ENZ} \quad (15)$$

Where $r_{enzloss}$ is the ratio of enzyme loss. Enzyme pool (ENZ) is modeled:

Biogeosciences Discuss., https://doi.org/10.5194/bg-2018-241
Manuscript under review for journal Biogeosciences
Discussion started: 13 June 2018

$$\frac{dENZ}{dt}=EPROD-ELOSS \quad (16)$$

Heterotrophic respiration (R_H) is an indispensable component of soil respiration (Bond-Lamberty and Thomson 2010), and closely coupled with soil nitrogen (N) mineralization that determines soil N availability, affecting gross primary production (GPP).

2.3 Model parameterization and validation

The variables and parameters of these microbial dynamics and their impacts on soil C decomposition were detailed in Allison et al 2010 (Table S5). Here we parameterized MIC-TEM for representative ecosystem types in northern high latitudes based on monthly net ecosystem productivity (NEP, gCm^{-2} mon^{-1}) measurements from AmeriFlux network (Davidson et al 2000) (Table S1). The results for model parameterization was presented in Fig. S2. Another set of level 4 gap-filled NEP data was used for model validation at site level (Table S2). The site-level monthly climate data of air temperature (℃), precipitation (mm) and cloudiness (%) were used to drive the model. Gridded MODIS NPP data from 2001 to 2010 were used to evaluate regional NPP simulation.

The parameterization was conducted with a global optimization algorithm SCE-UA (Shuffled complex evolution) (Duan et al 1994) to minimize the difference between the monthly simulated and measured NEE at these sites (Fig. S2). The cost function of the minimization is:

$$Obj = \sum_{i=1}^{k}(NEP_{obs,i} - NEP_{sim,i})^2 \quad (17)$$

Where $NEP_{obs,i}$ and $NEP_{sim,i}$ are the observed and simulated NEP, respectively. k is the number of data pairs for comparison. Other parameters used in MIC-TEM were default values from TEM

Biogeosciences Discuss., https://doi.org/10.5194/bg-2018-241
Manuscript under review for journal Biogeosciences
Discussion started: 13 June 2018

5.0 (Zhuang et al 2003, 2010). The optimized parameters were used for model validation and regional extrapolations.

2.4 Regional simulations

Two sets of regional simulations for the 20th century using MIC-TEM and TEM at a spatial resolution of 0.5 °latitude × 0.5 °longitude were conducted. Gridded forcing data of monthly air temperature, precipitation, and cloudiness were used, along with other ancillary inputs including historical atmospheric CO_2 concentrations, soil texture, elevation, and potential natural vegetation. Climatic inputs vary over time and space, whereas soil texture, elevation, and land cover data are assumed to remain unchanged throughout the 20th century, which only vary spatially. The transient climate data during the 20th century was organized from the Climatic Research Unit (CRU TS3.1) from the University of East Anglia (Harris et al 2014). The spatial-explicit data include potential natural vegetation (Melillo et al 1993), soil texture (Zhuang et al 2003) and elevation (Zhuang et al 2015).

Similarly, two sets of simulations were conducted driven with two contrasting climate change scenarios (RCP 2.6 and RCP 8.5) over the 21st century. The future climate change scenarios were derived from the HadGEM2-ES model, which is a member of CMIP5 project (https://esgf-node.llnl.gov/search/cmip5/). The future atmospheric CO_2 concentrations and climate forcing from each of the two climate change scenarios were used. The simulated NPP, R_H and NEP by both models (TEM 5.0 and MIC-TEM) were analyzed. The positive NEP represents a CO_2 sink from the atmosphere to terrestrial ecosystems, while a negative value represents a source of CO_2 from terrestrial ecosystems to the atmosphere.

Besides, in order to test the parameter uncertainty in our model, we conducted the regional simulations with 50 sets of parameters for both historical and future studies. The 50 sets of parameters were obtained according to the method in Tang and Zhuang 2008. The upper and lower bounds of the regional estimations were generated based on these simulations.

2.5 Sensitivity to initial soil carbon input

Future carbon dynamics can be affected by varying initial soil carbon amount. In the standard simulation of TEM, the initial soil carbon amount for transient simulations was obtained from equilibrium and spin-up periods directly for each grid cell in the region. To test the sensitivity to the initial soil carbon amount in transient simulations for the 21st century, we used empirical soil organic carbon data extracted from the Northern Circumpolar Soil Carbon Database (NCSCD) (Tarnocai et al 2009), as the initial soil carbon amount. The $0.5° \times 0.5°$ soil carbon data products for three different depths of 30cm, 100cm and 300cm were used. The sensitivity test was conducted for transient simulations under the RCP 2.6 and RCP 8.5 scenarios. To avoid the instability of C-N ratio caused by replacing the initial soil carbon pool with observed data at the beginning of transient period, initial soil nitrogen values were also generated based on the soil carbon data and corresponding C-N ratio map for transient simulations (Zhuang et al 2003, Raich and Schlesinger 1992).

3. Results

3.1 Model verification at site and regional levels

Biogeosciences Discuss., https://doi.org/10.5194/bg-2018-241
Manuscript under review for journal Biogeosciences
Discussion started: 13 June 2018

With the optimized parameters, MIC-TEM reproduces the carbon dynamics well for alpine tundra, boreal forest, temperate coniferous forest, temperate deciduous forest, grasslands and wet tundra with R^2 ranging from 0.70 for Ivotuk to 0.94 for Bartlett Experimental Forest (Fig. S3, table S3). In general, model performs better for forest ecosystems than for tundra ecosystems. The temporal NPP from 2001 to 2010 simulated by MIC-TEM and TEM were compared with MODIS NPP data (Fig. S4). Pearson correlation coefficients are 0.52 (MIC-TEM and MODIS) and 0.34 (TEM and MODIS). NPP simulated by MIC-TEM showed higher spatial correlation coefficients with MODIS data than TEM (Fig. S5). By considering more detailed microbial activities, the heterotrophic respiration is more adequately simulated using the MIC-TEM. The simulated differences in soil decomposition result in different levels of soil available nitrogen, which influences the nitrogen uptake by plants, the rate of photosynthesis and NPP. The spatial correlation coefficient between NPP simulated by MIC-TEM and MODIS is close to 1 in most study areas, suggesting the reliability of MIC-TEM at the regional scale.

3.2 Regional carbon dynamics during the 20th century

The equifinality of the parameters in MIC-TEM was considered in our ensemble regional simulations to measure the parameter uncertainty (Tang and Zhuang 2008). Here and below, the ensemble means and the inter-simulation standard deviations are shown for uncertainty measure, unless specified as others. These ensemble simulations indicated that the northern high latitudes act from a carbon source of 38.9 PgC to a carbon sink of 190.8 PgC by different ensemble members, with the mean of 64.2 ±21.4 Pg at the end of 20th century while the simulation with the optimized parameters estimates a regional carbon sink of 77.6 Pg with the interannual standard

deviation of 0.21 PgC yr^{-1} during the 20th century (Fig 1). Simulated regional NEP with optimized parameters using TEM and MIC-TEM showed an increasing trend throughout the 20th century except a slight decrease during the 1960s (Fig. 2). The Spatial distributions of NEP simulated by MIC-TEM for different periods in 20th century also show the increasing trend (Fig 3). Positive values of NEP represent sinks of CO_2 into terrestrial ecosystems, while negative values represent sources of CO_2 to the atmosphere. From 1900 onwards, both models estimated a regional carbon sink during the 20th century. With optimized parameters, TEM estimated higher NPP and R_H at 0.6 PgC yr^{-1} and 0.3 PgC yr^{-1} than MIC-TEM, respectively, at the end of the 20th century (Fig. 2). The MIC-TEM estimated a carbon sink increase from 0.64 to 0.83 $PgCyr^{-1}$ during the century while the estimated increase by TEM was much higher (0.28 $PgCyr^{-1}$) (Fig. 2). At the end of the century, MIC-TEM estimated NEP reached 1.0 $PgCyr^{-1}$ in comparison with TEM estimates of 0.3 $PgCyr^{-1}$. TEM estimated NPP and R_H are 0.5 $PgCyr^{-1}$ and 0.3 $PgCyr^{-1}$ higher, respectively. As a result, TEM estimated that the region accumulated 11.4 Pg more carbon than MIC-TEM. Boreal forests are a major carbon sink at 0.55 and 0.63 $PgCyr^{-1}$ estimated by MIC-TEM and TEM, respectively. Alpine tundra contributes the least sink. Overall, TEM overestimated the sink by 12.5% in comparison to MIC-TEM for forest ecosystems and 16.7% for grasslands. For wet tundra and alpine tundra, TEM overestimated about 20% and 33% in comparison with MIC-TEM, respectively (Table 1).

3.3 Regional carbon dynamics during the 21st century

Regional annual NPP and R_H increases under the RCP 8.5 scenario according to simulations with both models (Fig. 4). With optimized parameters, MIC-TEM estimated NPP increases from 9.2

in the 2000s to 13.2 $PgCyr^{-1}$ in the 2090s, while TEM predicted NPP is 2.0 $PgCyr^{-1}$ higher in the 2000s and 0.3 $PgCyr^{-1}$ higher in the 2090s (Fig. 4). Similarly, TEM also overestimated R_H by 1.7 $PgCyr^{-1}$ in the 2000s and 0.25 $PgCyr^{-1}$ higher in the 2090s, respectively (Fig. 4). As a result, the regional sink increases from 0.53 $PgCyr^{-1}$ in the 2000s, 1.4 $PgCyr^{-1}$ in the 2070s, then decreases to 1.1 $PgCyr^{-1}$ in the 2090s estimated by MIC-TEM (Fig. 4). Given the uncertainty in parameters, MIC-TEM predicted the region acts as a carbon sink ranging from 48.7 to 140.7 Pg, with the mean of 71.7 ±26.6 Pg at the end of 21st century, while the simulation with optimized parameters estimates a regional carbon source of 79.5 Pg with the interannual standard deviation of 0.37 PgC yr^{-1} during the 21st century (Fig 4). TEM predicted a similar trend for NEP, which overestimated the carbon sink with magnitude of 19.2 Pg compared with the simulation by MIC-TEM with optimized parameters. Under the RCP 2.6 scenario (Fig. 4), the increase of NPP and R_H is smaller from 2000 to 2100 compared to the simulation under the RCP 8.5. MIC-TEM predicted that NPP increases from 9.1 to 10.9 $PgCyr^{-1}$, TEM estimated 1.6 $PgCyr^{-1}$ higher at the beginning and 0.9 $PgCyr^{-1}$ higher in the end of the 21st century (Fig. 4). Consequently, MIC-TEM predicted NEP fluctuates between sinks and sources during the century, with a neutral before 2070, and a source between -0.2 - -0.3 Pg C yr^{-1} after the 2070s. As a result, the region acts as a carbon source of 1.6 Pg C with the interannual standard deviation of 0.24 PgC yr^{-1} estimated with MIC-TEM and a sink of 27.6 Pg C with the interannual standard deviation of 0.2 PgC yr^{-1} estimated with TEM during the century (Fig. 4). When considering the uncertainty source of parameters, MIC-TEM predicted the region acts from a carbon source of 64.8 Pg C to a carbon sink of 58.6 Pg C during the century with the mean of -3.3 ±20.3 Pg at the end of 21st century (Fig 4).

Biogeosciences Discuss., https://doi.org/10.5194/bg-2018-241
Manuscript under review for journal Biogeosciences
Discussion started: 13 June 2018

306

307 **3.4 Model sensitivity to initial soil carbon**

308 Under the RCP 2.6, without replacing the initial soil carbon with inventory-based estimates[1] in
309 model simulations, TEM estimated that the regional soil organic carbon (SOC) is 604.2 Pg C and
310 accumulates 12.1 Pg C during the 21st century. When using estimated soil carbon[1] within depths
311 of 30cm, 100cm and 300cm as initial pools in simulations, TEM predicted that regional SOC is
312 429.5, 689.3 and 1003.4 Pg C in 2000, and increases by 9.9, 16.0 and 22.8 Pg C at the end of the
313 21st century, and the regional cumulative carbon sink is 20.4, 34.0, and 48.1 Pg C, respectively
314 during the century. In contrast, using the same inventory-based SOC estimates, MIC-TEM
315 projected that the region acts from a cumulative carbon sink to a source at 0.7, 2.2, and 3.0 Pg C,
316 respectively. Under the RCP 8.5, both models predicted that the region acts as a carbon sink,
317 regardless of the magnitudes of initial soil carbon pools used, with TEM projected sink of 71.7,
318 120, and 155.6 Pg C and a much smaller cumulative sink of 65.4, 88.6, and 109.8 Pg C estimated
319 with MIC-TEM, respectively (Table 2).

320 **4. Discussion**

321 During the last few decades, a greening accompanying warming and rising atmospheric
322 CO_2 in the northern high latitudes (>45 °N) has been documented (McGuire et al 1995, McGuire
323 and Hobbie 1997, Chapin and Starfield 1997, Stow et al 2004, Callaghan et al 2005, Tape et al
324 2006, Giorgi et al 2006). The large stocks of carbon contained in the region (Tarnocai et al 2009)
325 are particularly vulnerable to climate change (Schuur et al 2008, McGuire et al 2009). To date,
326 the degree to which the ecosystems may serve as a source or a sink of C in the future are still

Biogeosciences Discuss., https://doi.org/10.5194/bg-2018-241
Manuscript under review for journal Biogeosciences
Discussion started: 13 June 2018

327 uncertain (McGuire et al 2009, Wieder et al 2013). Therefore, accurate models are essential for
328 predicting carbon–climate feedbacks in the future (Todd-Brown et al 2013). Our regional
329 simulations indicate the region is currently a carbon sink, which is consistent with many previous
330 studies (White et al 2000, Houghton et al 2007), and this sink will grow under the RCP 8.5
331 scenario, but shift to a carbon source under the RCP 2.6 scenario by 2100. MIC-TEM shows a
332 higher correlation between NPP and soil temperature (R=0.91) than TEM (R=0.82), suggesting
333 that MIC-TEM is more sensitive to environmental changes (Table S4).

334 Our regional estimates of carbon fluxes by MIC-TEM are within the uncertainty range
335 from other existing studies. For instance, Zhuang et al 2003 estimated the region as a sink of 0.9
336 $PgCyr^{-1}$ in extratropical ecosystems for the 1990s, which is similar to our estimation of 0.83
337 $PgCyr^{-1}$ by MIC-TEM. White et al 2000 estimated that, during the 1990s, regional NEP above
338 50 °N region is 0.46 $PgCyr^{-1}$ while Qian et al 2010 estimated that NEP increased from 0 to 0.3
339 $PgCyr^{-1}$ for the high-latitude region above 60 °N during last century, and reached 0.25 $PgCyr^{-1}$
340 during the 1990s. White et al 2000 predicted that, from 1850 to 2100, the region accumulated
341 134 PgC in terrestrial ecosystems, in comparison with our estimates of 77.6 PgC with MIC-TEM
342 and 89 PgC with TEM. Our projection of a weakening sink during the second half of the 21st
343 century is consistent with previous model studies (Koven et al 2011, Schaphoff et al 2013). Our
344 predicted trend of NEP is very similar to the finding of White et al 2000, indicating that NEP
345 increases from 0.46 $PgCyr^{-1}$ in the 2000s and reaches 1.5 $PgCyr^{-1}$ in the 2070s, then decreases to
346 0.6 $PgCyr^{-1}$ in the 2090s.

347 The MIC-TEM simulated NEP generally agrees with the observations. However, model
348 simulations still deviate from the observed data, especially for tundra ecosystems. The deviation

may be due to the uncertainty or errors in the observed data, which do not well constrain the model parameters. Uncertain driving data such as temperature and precipitation are also a source of uncertainty for transient simulations. In addition, we assumed that vegetation will not change during the transient simulation. However, over the past few decades in the northern high latitudes, temperature increases have led to vegetation changes (Hansen et al 2006), including latitudinal treeline advance (Lloyd et al 2005) and increasing shrub density (Sturm et al 2001). Vegetation can shift from one type to another because of competition for light, N and water (White et al 2000). For example, needleleaved trees tend to replace tundra gradually in response to warming. In some areas, forests even moved several hundreds of kilometers within 100 years (Gear and Huntley 1991). The vegetation changes will affect carbon cycling in these ecosystems. In addition, we have not yet considered the effects of management of agriculture lands (Cole et al 1997), but Zhuang et al 2003 showed that the changes in agricultural land use in northern high latitudes have been small.

The largest limitation to this study is that we have not explicitly considered the fire effects. Warming in the northern high latitudes could favor fire in its frequency, intensity, seasonality and extent (Kasischke and Turetsky 2006, Johnstone and Kasischke 2005, Soja et al 2007, Randerson,et al 2006, Bond-Lamberty et al 2007). Fire has profound effects on northern forest ecosystems, altering the N cycle and water and energy exchanges between the atmosphere and ecosystems. Increase in wildfires will destroy most of above-ground biomass and consume organic soils, resulting in less carbon uptake by vegetation (Harden et al 2000), leading to a net release of carbon in a short term. However, a suite of biophysical mechanisms of ecosystems including post-fire increase in the surface albedo and rates of biomass accumulation may in turn,

exert a negative feedback to climate warming (Amiro et al 2006, Goetz et al 2007), further influence the carbon exchanges between ecosystems and the atmosphere.

Moreover, carbon uptake in land ecosystems depends on new plant growth, which connects tightly with the availability of nutrients such as mineral nitrogen. Recent studies have shown that when soil nitrogen is in short supply, most terrestrial plants would form symbiosis relationships with fungi; hyphae provides nitrogen to plants, in return, plants provide sugar to fungi (Hobbie and Hobbie 2008, 2006, Schimel and Hättenschwiler 2007). This symbiosis relationship has not been considered in our current modeling, which may lead to a large uncertainty in our quantification of carbon and nitrogen dynamics.

Shift in microbial community structure was not considered in our model, which could affect the temperature sensitivity of heterotrophic respiration (Stone et al 2012). Michaelis-Menten constant (K_m) could also adapt to climate warming, and it may increase more significantly with increasing temperature in cold-adapted enzymes than in warm-adapted enzymes (German et al 2012, Somero et al 2004, Dong and Somero 2009). Carbon use efficiency (CUE) is also a controversial parameter in our model. Empirical studies in soils suggest that microbial CUE declines by at least 0.009 $°C^{-1}$ (Steinweg et al 2008), while other studies find that CUE is invariant with temperature (López-Urrutia and Morán 2007). Another key microbial trait lacking in our modeling is microbial dormancy (He et al 2015). Dormancy is a common, bet-hedging strategy used by microorganisms when environmental conditions limit their growth and reproduction (Lennon and Jones 2011). Microorganisms in dormancy are not able to drive biogeochemical processes such as soil CO_2 production, and therefore, only active microorganisms should be involved in utilizing substrates in soils (Blagodatskaya and Kuzyakov

2013). Many studies have indicated that soil respiration responses to environmental conditions are more closely associated with the active portion of microbial biomass than total microbial biomass (Hagerty et al 2014, Schimel and Schaeffer 2012, Steinweg et al 2013). Thus, the ignorance of microbial dormancy could fail to distinguish microbes with different physiological states, introducing uncertainties to our carbon estimation.

5. Conclusions

This study used a more detailed microbial biogeochemistry model to investigate the carbon dynamics in the region for the past and this century. Regional simulations using MIC-TEM indicated that, over the 20th century, the region is a sink of 77.6 Pg. This sink could reach to 79.5 Pg under the RCP 8.5 scenario or shift to a carbon source of 1.6 Pg under the RCP 2.6 scenario during 21st century. On the other hand, traditional TEM overestimated the carbon sink under the RCP 8.5 scenario with magnitude of 19.2 Pg than MIC-TEM, and predicted this region acting as carbon sink with magnitude of 27.6 Pg under the RCP 2.6 scenario during 21st century. Using recent soil carbon stock data as initial soil carbon in model simulations, the region was estimated to shift from a carbon sink to a source, with total carbon release at 0.7- 3 Pg by 2100 depending on initial soil carbon pools at different soil depths under the RCP 2.6 scenario. In contrast, the region acts as a carbon sink at 55.4 - 99.8 Pg C in the 21st century under RCP 8.5 scenario. Without considering more detailed microbial processes, models estimated that the region acts as a carbon sink under both scenarios. Under the RCP 2.6 scenario, the cumulative sink ranges from 9.9 to 22.8 Pg C. Under the RCP 8.5 scenario, the cumulative sink is even larger at 71.7 - 155.6 Pg C. This study indicated that more detailed microbial physiology-based biogeochemistry models estimate carbon dynamics very differently from using a relatively

simple microbial decomposition-based model. The comparison with satellite products or other estimates for the 20th century suggests that the more detailed microbial decomposition shall be considered to adequately quantify C dynamics in northern high latitudes.

Acknowledgments

This research was supported by a NSF project (IIS-1027955), a DOE project (DE-SC0008092), and a NASA LCLUC project (NNX09AI26G) to Q. Z. We acknowledge the Rosen High Performance Computing Center at Purdue for computing support. We thank the National Snow and Ice Data center for providing Global Monthly EASE-Grid Snow Water Equivalent data, National Oceanic and Atmospheric Administration for North American Regional Reanalysis (NARR), and Hugelius and his group by making available pan-Arctic permafrost soil C maps. We also acknowledge the World Climate Research Programme's Working Group on Coupled Modeling Intercomparison Project CMIP5, and we thank the climate modeling groups for producing and making available their model output. The data presented in this paper can be accessed through our research website (http://www.eaps.purdue.edu/ebdl/)

References

Tarnocai, C. et al. Soil organic carbon pools in the northern circumpolar permafrost region, Global Biogeochem. Cycles, 23, GB2023, doi:10.1029/2008GB003327 (2009).

Serreze, M. C. and Francis, J. A. The Arctic on the fast track of change. Weather, 61: 65–69. doi:10.1256/wea.197.05 (2006).

Holland, M.M. & Bitz, C.M. Climate Dynamics. 21: 221. doi:10.1007/s00382-003-0332-6 (2003)

Davidson, E. A., & Janssens, I. A. Temperature sensitivity of soil carbon decomposition and feedbacks to climate change. *Nature*, *440*(7081), 165-173 (2006).

Christensen, J.H. & Christensen, O.B. Climatic Change. 81(Suppl 1): 7. doi:10.1007/s10584-006-9210-7 (2007).

Oechel, W. C. et al. Acclimation of ecosystem CO_2 exchange in the Alaskan Arctic in response to decadal climate warming. *Nature*, *406*(6799), 978-981 (2000).

Mack, M. C. et al. Ecosystem carbon storage in arctic tundra reduced by long-term nutrient fertilization. *Nature*, *431*(7007), 440-443 (2004).

Hobbie, S. E. et al. Plant and Soil. 242: 163. doi:10.1023/A:1019670731128 (2002).

Davidson, E. A. et al. Biogeochemistry: soil warming and organic carbon content. *Nature*, *408*(6814), 789-790 (2000).

Jobbágy, E. G. and Jackson, R. B. THE VERTICAL DISTRIBUTION OF SOIL ORGANIC CARBON AND ITS RELATION TO CLIMATE AND VEGETATION. Ecological Applications, 10: 423–436. doi:10.1890/1051-0761(2000)010[0423:TVDOSO]2.0.CO;2 (2000).

Hayes, D. J. et al. The impacts of recent permafrost thaw on land–atmosphere greenhouse gas exchange. *Environmental Research Letters*, *9*(4), 045005 (2014).

Raich, J. W. and Schlesinger, W. H. The global carbon dioxide flux in soil respiration and its relationship to vegetation and climate. Tellus B, 44: 81–99. doi:10.1034/j.1600-0889.1992.t01-1-00001.x (1992).

McGuire, A. D. et al. Interactions between carbon and nitrogen dynamics in estimating net primary productivity for potential vegetation in North America, Global Biogeochem. Cycles, 6(2), 101–124, doi:10.1029/92GB00219 (1992).

Zhuang, Q. et al. Incorporation of a permafrost model into a large-scale ecosystem model: Evaluation of temporal and spatial scaling issues in simulating soil thermal dynamics, J.

Geophys. Res., 106(D24), 33649–33670, doi:10.1029/2001JD900151 (2001).

Zhuang, Q. et al. Modeling soil thermal and carbon dynamics of a fire chronosequence in interior Alaska, J. Geophys. Res., 107, 8147, doi:10.1029/2001JD001244, 2002. [printed 108(D1), 2003] (2002).

Zhuang, Q. et al. Carbon cycling in extratropical terrestrial ecosystems of the Northern Hemisphere during the 20th century: a modeling analysis of the influences of soil thermal dynamics. Tellus B, 55: 751–776. doi:10.1034/j.1600-0889.2003.00060.x (2003).

Zhuang, Q. et al. Carbon dynamics of terrestrial ecosystems on the Tibetan Plateau during the 20th century: an analysis with a process-based biogeochemical model. Global Ecology and Biogeography, 19: 649–662. doi:10.1111/j.1466-8238.2010.00559.x (2010)

Zhuang, Q. et al. Response of global soil consumption of atmospheric methane to changes in atmospheric climate and nitrogen deposition, Global Biogeochem. Cycles, 27, 650–663, doi:10.1002/gbc.20057 (2013).

Running, S. W., & Coughlan, J. C. A general model of forest ecosystem processes for regional applications I. Hydrologic balance, canopy gas exchange and primary production processes. *Ecological modelling*, *42*(2), 125-154 (1988).

Potter, C. S. et al. Terrestrial ecosystem production: a process model based on global satellite and surface data. *Global Biogeochemical Cycles*, *7*(4), 811-841 (1993).

Parton, W. J. et al. A general model for soil organic matter dynamics: sensitivity to litter chemistry, texture and management. *Quantitative modeling of soil forming processes*, (quantitativemod), 147-167 (1994).

Knorr, W. Annual and interannual CO_2 exchanges of the terrestrial biosphere: process-based simulations and uncertainties. Global Ecology and Biogeography, 9: 225–252. doi:10.1046/j.1365-2699.2000.00159.x (2000).

Todd-Brown, K.E.O. et al. Biogeochemistry109: 19. doi:10.1007/s10533-011-9635-6 (2012).

McGuire, A. D. et al. An assessment of the carbon balance of Arctic tundra: comparisons among observations, process models, and atmospheric inversions. *Biogeosciences Discussions*, *9*, 4543 (2012).

Schimel, J.P. Soil carbon: microbes and global carbon. *Nature Climate Change*, *3*(10), 867-868 (2013).

Todd-Brown, K. E. et al. Causes of variation in soil carbon simulations from CMIP5 Earth system models and comparison with observations. *Biogeosciences*, *10*(3) (2013).

Ciais, P. et al. Carbon and Other Biogeochemical Cycles. In: Climate Change 2013: The Physical Science Basis. Contribution of Working Group I to the Fifth Assessment Report of the Intergovernmental Panel on Climate Change [Stocker, T.F., D. Qin, G.-K. Plattner, M. Tignor, S.K. Allen, J. Boschung, A. Nauels, Y. Xia, V. Bex and P.M. Midgley (eds.)]. Cambridge University Press, Cambridge, United Kingdom and New York, NY, USA (2013).

Wieder, W. R. et al. Global soil carbon projections are improved by modelling microbial processes. *Nature Climate Change*, *3*(10), 909-912 (2013).

Schmidt, M. W. et al. Persistence of soil organic matter as an ecosystem property. *Nature*, *478*(7367), 49-56 (2011).

Hanson, P. et al. Biogeochemistry 48: 115. doi:10.1023/A:1006244819642 (2000).

Bond-Lamberty, B., & Thomson, A. Temperature-associated increases in the global soil respiration record. *Nature*, *464*(7288), 579-582 (2010).

Cook, F. J., & Orchard, V. A. Relationships between soil respiration and soil moisture. *Soil Biology and Biochemistry*, *40*(5), 1013-1018 (2008).

Hao, G. et al. Climatic Change 133: 695. doi:10.1007/s10584-015-1490-3 (2015).

Lawrence, D. M., et al. Parameterization improvements and functional and structural advances in Version 4 of the Community Land Model, J. Adv. Model. Earth Syst., 3, M03001, doi:10.1029/2011MS00045 (2011).

Schimel, J. P., & Weintraub, M. N. The implications of exoenzyme activity on microbial carbon and nitrogen limitation in soil: a theoretical model. *Soil Biology and Biochemistry*, *35*(4), 549-563 (2003).

Barichivich, J. et al. Large-scale variations in the vegetation growing season and annual cycle of atmospheric CO_2 at high northern latitudes from 1950 to 2011. Glob Change Biol, 19: 3167–3183. doi:10.1111/gcb.12283 (2013).

Allison, S. D., & Martiny, J. B. Resistance, resilience, and redundancy in microbial communities. *Proceedings of the National Academy of Sciences*, *105*(Supplement 1), 11512-11519 (2008).

Allison, S. D. et al. Soil-carbon response to warming dependent on microbial physiology. *Nature Geoscience*, *3*(5), 336-340 (2010).

Melillo, J. M. et al. Global climate change and terrestrial net primary production. *Nature*, *363*(6426), 234-240 (1993).

McGuire, A. D. et al. Equilibrium responses of soil carbon to climate change: empirical and process-based estimates. *Journal of Biogeography*, 785-796 (1995).

McGuire, A. D., & Hobbie, J. E. Global climate change and the equilibrium responses of carbon storage in arctic and subarctic regions. In *Modeling the Arctic system: A workshop report on the state of modeling in the Arctic System Science program* (pp. 53-54) (1997).

Chapin, F.S. & Starfield, A.M. Climatic Change 35: 449. doi:10.1023/A:1005337705025 (1997).

Stow, D. A. et al. Remote sensing of vegetation and land-cover change in Arctic Tundra Ecosystems. *Remote sensing of environment*, *89*(3), 281-308 (2004).

Callaghan, T. V. et al. Arctic tundra and polar desert ecosystems. *Arctic climate impact assessment*, *1*, 243-352 (2005).

TAPE, K. et al. The evidence for shrub expansion in Northern Alaska and the Pan-Arctic. Global Change Biology, 12: 686–702. doi:10.1111/j.1365-2486.2006.01128.x (2006).

Giorgi, F. Regional climate modeling: Status and perspectives. In *Journal de Physique IV (Proceedings)* (Vol. 139, pp. 101-118). EDP sciences (2006).

Schuur, E. A. et al. Vulnerability of permafrost carbon to climate change: Implications for the global carbon cycle. *BioScience*, *58*(8), 701-714 (2008).

Zimov, S. A. et al. Permafrost and the global carbon budget. *Science*, *312*(5780), 1612-1613 (2006).

McGuire, A. D. et al. Sensitivity of the carbon cycle in the Arctic to climate change. Ecological Monographs, 79: 523–555. doi:10.1890/08-2025.1(2009).

White, A. et al. The high-latitude terrestrial carbon sink: a model analysis. Global Change Biology, 6: 227–245. doi:10.1046/j.1365-2486.2000.00302.x (2000).

Houghton, R. A. Balancing the global carbon budget. *Annu. Rev. Earth Planet. Sci.*, *35*, 313-347 (2007).

Qian, H. et al. Enhanced terrestrial carbon uptake in the Northern High Latitudes in the 21st century from the Coupled Carbon Cycle Climate Model Intercomparison Project model projections. Global Change Biology, 16: 641–656. doi:10.1111/j.1365-2486.2009.01989.x (2010).

Koven, C. D. et al. Permafrost carbon-climate feedbacks accelerate global warming. *Proceedings of the National Academy of Sciences*, *108*(36), 14769-14774 (2011).

Schaphoff, S. et al. Contribution of permafrost soils to the global carbon budget. *Environmental Research Letters*, *8*(1), 014026 (2013).

Hansen, J. et al. Global temperature change. *Proceedings of the National Academy of Sciences*, *103*(39), 14288-14293 (2006).

Lloyd, A. H. ECOLOGICAL HISTORIES FROM ALASKAN TREE LINES PROVIDE INSIGHT INTO FUTURE CHANGE. Ecology, 86: 1687–1695. doi:10.1890/03-0786 (2005).

Sturm, M. et al. Climate change: increasing shrub abundance in the Arctic. *Nature*, *411*(6837), 546-547 (2001).

Gear, A. J., & Huntley, B. Rapid changes in the range limits of Scots pine 4000 years ago. *Science*, *251*(4993), 544-548 (1991).

Cole, C. et al. Nutrient Cycling in Agroecosystems 49: 221. doi:10.1023/A:1009731711346 (1997).

Kasischke, E. S., and M. R. Turetsky. Recent changes in the fire regime across the North American boreal region—Spatial and temporal patterns of burning across Canada and Alaska, Geophys. Res. Lett., 33, L09703, doi:10.1029/2006GL025677 (2006).

Johnstone, J. F., & Kasischke, E. S. Stand-level effects of soil burn severity on postfire regeneration in a recently burned black spruce forest. *Canadian Journal of Forest Research*, *35*(9), 2151-2163 (2005).

Soja, A. J. et al. Climate-induced boreal forest change: predictions versus current observations. *Global and Planetary Change*, *56*(3), 274-296 (2007).

Randerson, J. T. et al. The impact of boreal forest fire on climate warming. *science*, *314*(5802), 1130-1132 (2006).

Bond-Lamberty, B. et al. Fire as the dominant driver of central Canadian boreal forest carbon balance. *Nature*, *450*(7166), 89-92 (2007).

Harden, J. W. et al. The role of fire in the boreal carbon budget. Global Change Biology, 6: 174–184. doi:10.1046/j.1365-2486.2000.06019.x (2000).

Amiro, B. D. et al. The effect of post-fire stand age on the boreal forest energy balance. *Agricultural and Forest Meteorology*, *140*(1), 41-50 (2006).

Goetz, S. J. et al. Ecosystem responses to recent climate change and fire disturbance at northern high latitudes: observations and model results contrasting northern Eurasia and North America. *Environmental Research Letters*, *2*(4), 045031 (2007).

Hobbie, E.A. & Hobbie, J.E. Ecosystems 11: 815. doi:10.1007/s10021-008-9159-7 (2008).

Hobbie, J. E. and Hobbie, E. A. ^{15}N IN SYMBIOTIC FUNGI AND PLANTS ESTIMATES NITROGEN AND CARBON FLUX RATES IN ARCTIC TUNDRA. Ecology, 87: 816–822. doi:10.1890/0012-9658(2006)87[816:NISFAP]2.0.CO;2 (2006).

Schimel, J. P., & Hättenschwiler, S. Nitrogen transfer between decomposing leaves of different N status. *Soil Biology and Biochemistry*, *39*(7), 1428-1436 (2007).

Stone, M. M. et al. Temperature sensitivity of soil enzyme kinetics under N-fertilization in two temperate forests. Glob Change Biol, 18: 1173–1184. doi:10.1111/j.1365-2486.2011.02545.x (2012).

German, D. P. et al. The Michaelis–Menten kinetics of soil extracellular enzymes in response to temperature: a cross-latitudinal study. Glob Change Biol, 18: 1468–1479. doi:10.1111/j.1365-2486.2011.02615.x (2012).

Somero, G. N. Adaptation of enzymes to temperature: searching for basic "strategies". *Comparative Biochemistry and Physiology Part B: Biochemistry and Molecular Biology*, *139*(3), 321-333 (2004).

Dong, Y., & Somero, G. N. Temperature adaptation of cytosolic malate dehydrogenases of limpets (genus Lottia): differences in stability and function due to minor changes in sequence correlate with biogeographic and vertical distributions. *Journal of Experimental Biology*, *212*(2), 169-177 (2009).

Steinweg, J. M. et al. Patterns of substrate utilization during long-term incubations at different temperatures. *Soil Biology and Biochemistry*, *40*(11), 2722-2728.

López-Urrutia, Á. and Morán, X. A. G. (2007), resource limitation of bacterial production distorts the temperature dependence of oceanic carbon cycling. Ecology, 88: 817–822. doi:10.1890/06-1641(2008).

He, Y. et al. Incorporating microbial dormancy dynamics into soil decomposition models to improve quantification of soil carbon dynamics of northern temperate forests, J. Geophys. Res. Biogeosci., 120, 2596–2611, doi:10.1002/2015JG003130 (2015).

Lennon, J. T., & Jones, S. E. Microbial seed banks: the ecological and evolutionary implications of dormancy. *Nature Reviews Microbiology*, *9*(2), 119-130 (2011).

Blagodatskaya, E., & Kuzyakov, Y. Active microorganisms in soil: critical review of estimation criteria and approaches. *Soil Biology and Biochemistry*, *67*, 192-211 (2013).

Hagerty, S. B. et al. Accelerated microbial turnover but constant growth efficiency with warming in soil. *Nature Climate Change*, *4*(10), 903-906 (2014).

Schimel, J. P., & Schaeffer, S. M. Microbial control over carbon cycling in soil. *Frontiers in microbiology*, *3 (2012)*.

Steinweg, J. M. et al. Microbial responses to multi-factor climate change: effects on soil enzymes. *Frontiers in microbiology*, *4 (2013)*.

Duan, Q. et al. Optimal use of the SCE-UA global optimization method for calibrating watershed models. *Journal of hydrology*, *158*(3-4), 265-284 (1994).

Harris, I. et al. Updated high-resolution grids of monthly climatic observations – the CRU TS3.10 Dataset. Int. J. Climatol., 34: 623–642. doi:10.1002/joc.3711 (2014).

Zhuang, Q. et al. Influence of changes in wetland inundation extent on net fluxes of carbon dioxide and methane in northern high latitudes from 1993 to 2004. *Environmental Research Letters*, *10*(9), 095009 (2015).

Tang, J., and Q. Zhuang. 2008. Equifinality in parameterization of process-based biogeochemistry models: A significant uncertainty source to the estimation of regional carbon dynamics. Journal of Geophysical Research: Biogeosciences. doi: 10.1029/2008JG000757

Author contributions. Q.Z. designed the study. J.Z. conducted model development, simulation and analysis. J.Z. and Q. Z. wrote the paper.

Competing financial interests. The submission has no competing financial interests.

Materials & Correspondence. Correspondence and material requests should be addressed to qzhuang@purdue.edu.

Biogeosciences Discuss., https://doi.org/10.5194/bg-2018-241
Manuscript under review for journal Biogeosciences
Discussion started: 13 June 2018

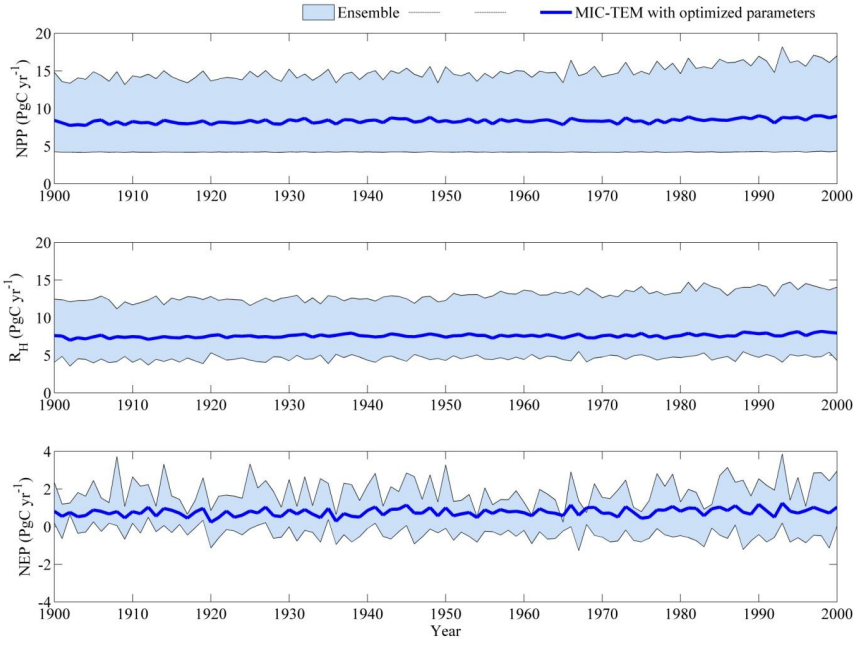

Figure 1. Simulated annual net primary production (NPP, top panel), heterotrophic respiration (R_H, center panel) and net ecosystem production (NEP, bottom panel) by MIC-TEM with ensemble of parameters.

Biogeosciences Discuss., https://doi.org/10.5194/bg-2018-241
Manuscript under review for journal Biogeosciences
Discussion started: 13 June 2018

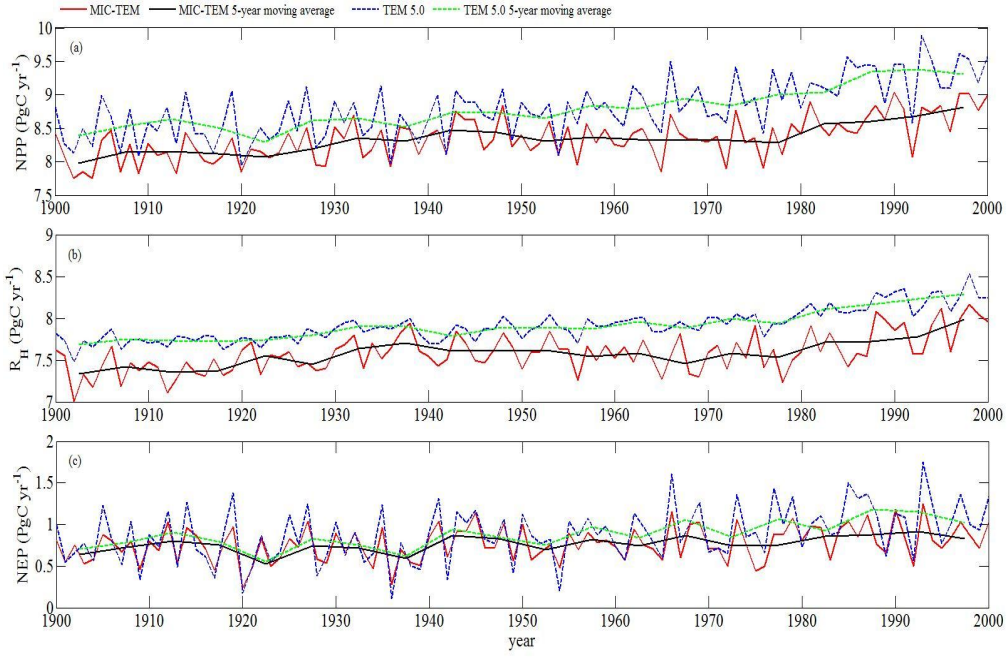

Figure 2. Simulated annual net primary production (NPP, top panel), heterotrophic respiration (R_H, center panel) and net ecosystem production (NEP, bottom panel) by MIC-TEM and TEM, respectively.

Biogeosciences Discuss., https://doi.org/10.5194/bg-2018-241
Manuscript under review for journal Biogeosciences
Discussion started: 13 June 2018

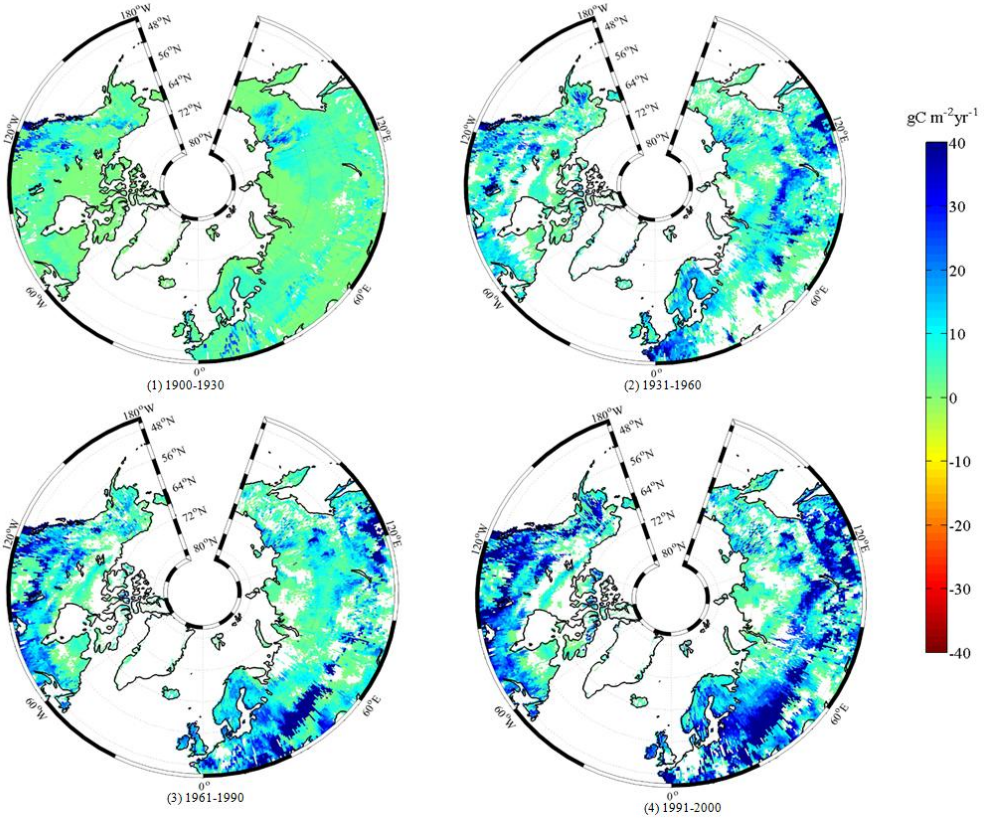

Figure 3. Spatial distribution of NEP simulated by MIC-TEM for the periods: (1) 1900-1930, (2) 1931-1960, (3) 1961-1990, and (4) 1991-2000. Positive values of NEP represent sinks of CO_2 into terrestrial ecosystems, while negative values represent sources of CO_2 to the atmosphere.

Biogeosciences Discuss., https://doi.org/10.5194/bg-2018-241
Manuscript under review for journal Biogeosciences
Discussion started: 13 June 2018

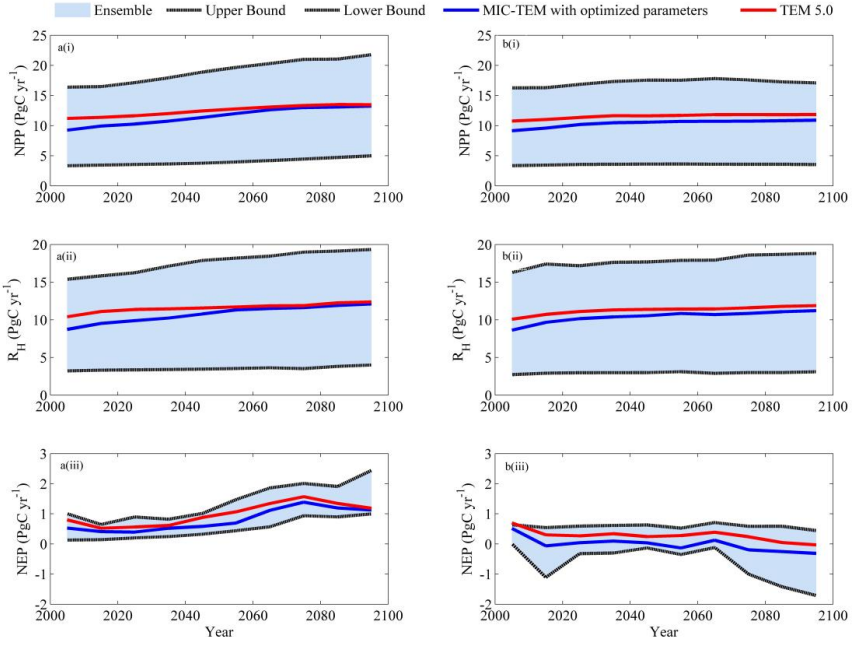

Figure 4. Predicted changes in carbon fluxes: (i) NPP, (ii) R_H, and (iii) NEP for all land areas north of 45 °N in response to transient climate change under (a) RCP 8.5 scenario and (b) RCP 2.6 scenario with MIC-TEM and TEM 5.0, respectively. The decadal running mean is applied. The grey area represents the upper and lower bounds of simulations.

Biogeosciences Discuss., https://doi.org/10.5194/bg-2018-241
Manuscript under review for journal Biogeosciences
Discussion started: 13 June 2018

Table 1. Partitioning of average annual net ecosystem production (as Pg C per year) for six vegetation types during the 20th century

	MIC-TEM (PgC yr^{-1})	TEM 5.0 (PgC y^{-1})
Alpine tundra	0.03	0.04
Boreal forest	0.39	0.45
Conifer forest	0.09	0.09
Deciduous forest	0.16	0.18
Grassland	0.06	0.07
Wet tundra	0.05	0.06
Total	0.78	0.89

Biogeosciences Discuss., https://doi.org/10.5194/bg-2018-241
Manuscript under review for journal Biogeosciences
Discussion started: 13 June 2018

Table 2. Increasing of SOC, vegetation carbon (VGC), soil organic nitrogen (SON), vegetation nitrogen (VGN) from 1900 to 2000, and total carbon storage during the 21st century predicted by two models with observed soil carbon data of three different depths under (a) RCP 2.6 and (b) RCP 8.5.

(a)

Model	Units: Pg	Without (control)	30cm	100cm	300cm
TEM 5.0	SOC/SON in 2000	604.2/27.0	429.5/19.0	689.3/31.6	1003.4/46.2
	Increase of SOC during the 21st century	12.1	9.9	16.0	22.8
	VGC/VGN in 2000	318.3/1.48	238.4/1.05	394.2/1.80	556.7/2.53
	Increase of VGC during the 21st century	15.5	10.5	18.0	25.3
	Increase of total carbon storage during the 21st century	27.6	20.4	34.0	48.1
MIC-TEM	SOC/SON in 2000	591.5/26.8	420.3/18.6	686.0/31.2	990.7/45.3
	Increase of SOC during the 21st century	-2.0	-1.2	-2.4	-2.9
	VGC/VGN in 2000	309.7/1.42	230.1/1.02	374.4/1.71	548.6/2.45
	Increase of VGC during the 21st century	0.4	0.5	0.2	-0.1
	Increase of total carbon storage during the 21st century	-1.6	-0.7	-2.2	-3.0

(b)

Biogeosciences Discuss., https://doi.org/10.5194/bg-2018-241
Manuscript under review for journal Biogeosciences
Discussion started: 13 June 2018

Model	Units: Pg	Without (control)	30cm	100cm	300cm
TEM 5.0	SOC/SON in 2000	610.2 /27.9	431.9/19.1	693.8/31.8	1007.1/46.4
	Increase of SOC during the 21st century	44.2	33.0	56.5	74.6
	VGC/VGN in 2000	324.9/1.50	242.1/1.07	399.6/1.83	570.2/2.57
	Increase of VGC during the 21st century	54.5	38.7	63.5	81.0
	Increase of total carbon storage during the 21st century	98.7	71.7	120.0	155.6
MIC-TEM	SOC/SON in 2000	596.0/27.1	424.6/18.8	689.1/31.5	995.5/46.1
	Increase of SOC during the 21st century	33.3	27.4	36.9	42.9
	VGC/VGN in 2000	316.0/1.44	233.5/1.02	380.0/1.72	568.3/2.56
	Increase of VGC during the 21st century	46.2	37.0	51.7	56.9
	Increase of total carbon storage during the 21st century	79.5	65.4	88.6	109.8